

Determination of the strong coupling constant based on NNLO+NLLA results for hadronic event shapes and a study of hadronisation corrections

*G. Dissertori*¹, *A. Gehrmann–De Ridder*², *T. Gehrmann*³, *E.W.N. Glover*⁴, *G. Heinrich*⁴, *M. Jaquier*³, *G. Luisoni*³, *H. Stenzel*⁵

¹ Institute for Particle Physics, ETH Zurich, CH-8093 Zurich, Switzerland

² Institute for Theoretical Physics, ETH Zurich, CH-8093 Zurich, Switzerland

³ Institut für Theoretische Physik, Universität Zürich, CH-8057 Zürich, Switzerland

⁴ Institute for Particle Physics Phenomenology, University of Durham, Durham, DH1 3LE, UK

⁵ II. Physikalisches Institut, Justus-Liebig Universität Giessen, D-35392 Giessen, Germany

Abstract

We report on a determination of the strong coupling constant from a fit of QCD predictions for six event-shape variables, calculated at next-to-next-to-leading order (NNLO) and matched to resummation in the next-to-leading-logarithmic approximation (NLLA). We use data collected by ALEPH at centre-of-mass energies between 91 and 206 GeV. We also investigate the role of hadronisation corrections, using both Monte Carlo generator predictions and analytic models to parametrise non-perturbative power corrections.

1. INTRODUCTION

Event-shape observables describe topological properties of hadronic final states without the need to define jets, quantifying the structure of an event by a single measure. This class of observables is also interesting because it shows a rather strong sensitivity to hadronisation effects, at least in phase-space regions characterised by soft and collinear gluon radiation, which correspond to certain limits for each event-shape variable.

Event-shape distributions in e^+e^- annihilation have been measured with high accuracy by a number of experiments, most of them at LEP at centre-of-mass energies between 91 and 206 GeV [1, 2, 3, 4, 5, 6, 7, 8, 9, 10, 11, 12, 13, 14, 15]. Mean values and higher moments also have been measured by several experiments, most extensively by JADE [16, 17] and OPAL [7].

For a long time, the theoretical state-of-the-art description of event-shape distributions over the full kinematic range was based on the matching of the next-to-leading-logarithmic approximation (NLLA) [18] onto the fixed next-to-leading order (NLO) calculation [19, 20, 21]. Recently, NNLO results for event-shape distributions became available [22, 23, 24] and lead to the first determination of the strong coupling constant using NNLO predictions for hadronic event shapes in e^+e^- annihilations [25]. Soon after, the matching of the resummed result in the next-to-leading-logarithmic approximation onto the NNLO calculation has been performed [26] in the so-called $\ln R$ -matching scheme [18]. Based on these results, a determination of the strong coupling constant using matched NNLO+NLLA predictions for hadronic event shapes has been carried out [27], together with a detailed investigation of hadronisation corrections. Next-to-leading order electroweak corrections to event-shape distributions in e^+e^- annihilation were also computed very recently [28].

A similar NNLO+NLLA study based on JADE data was done in [29], while other NNLO determinations of $\alpha_s(M_Z)$ based on only the thrust distribution were presented in [30, 31].

Apart from distributions of event-shape observables, one can also study mean values and higher moments, which are now available at NNLO accuracy [32, 33]. Moments are particularly attractive in view of studying non-perturbative hadronisation corrections to event shapes. In ref. [34], NNLO perturbative QCD predictions have been combined with non-perturbative power corrections in a dispersive model [35, 36, 37, 38]. The resulting theoretical expressions have been compared to experimental data

from JADE and OPAL, and new values for both $\alpha_s(M_Z)$ and α_0 , the effective coupling in the non-perturbative regime, have been determined.

The two approaches – estimating the hadronisation corrections by general purpose Monte Carlo programs or modelling power corrections analytically – shed light on the subject of hadronisation corrections from two different sides and lead to some interesting insights which will be summarised in the following.

2. THEORETICAL FRAMEWORK

We have studied the six event-shape observables thrust T [39] (respectively $\tau = 1 - T$), heavy jet mass M_H [40], wide and total jet broadening B_W and B_T [41], C -parameter [42, 43] and the two-to-three-jet transition parameter in the Durham algorithm, Y_3 [44, 45]. The definitions of these variables, which we will denote collectively as y in the following, are summarised e.g. in [23].

2.1 event-shape distributions

The fixed-order QCD description of event-shape distributions starts from the perturbative expansion

$$\frac{1}{\sigma_0} \frac{d\sigma}{dy}(y, Q, \mu) = \bar{\alpha}_s(\mu) \frac{dA}{dy}(y) + \bar{\alpha}_s^2(\mu) \frac{dB}{dy}(y, x_\mu) + \bar{\alpha}_s^3(\mu) \frac{dC}{dy}(y, x_\mu) + \mathcal{O}(\bar{\alpha}_s^4), \quad (1)$$

where

$$\bar{\alpha}_s = \frac{\alpha_s}{2\pi}, \quad x_\mu = \frac{\mu}{Q},$$

and where A , B and C are the perturbatively calculated coefficients [23] at LO, NLO and NNLO.

All coefficients are normalised to the tree-level cross section σ_0 for $e^+e^- \rightarrow q\bar{q}$. For massless quarks, this normalisation cancels all electroweak coupling factors, and the dependence of (1) on the collision energy is only through α_s and x_μ . Predictions for the experimentally measured event-shape distributions are then obtained by normalising to σ_{had} as

$$\frac{1}{\sigma_{\text{had}}} \frac{d\sigma}{dy}(y, Q, \mu) = \frac{\sigma_0}{\sigma_{\text{had}}(Q, \mu)} \frac{1}{\sigma_0} \frac{d\sigma}{dy}(y, Q, \mu). \quad (2)$$

In all expressions, the scale dependence of α_s is determined according to the three-loop running:

$$\alpha_s(\mu^2) = \frac{2\pi}{\beta_0 L} \left(1 - \frac{\beta_1}{\beta_0^2} \frac{\ln L}{L} + \frac{1}{\beta_0^2 L^2} \left(\frac{\beta_1^2}{\beta_0^2} (\ln^2 L - \ln L - 1) + \frac{\beta_2}{\beta_0} \right) \right), \quad (3)$$

where $L = 2 \ln(\mu/\Lambda_{\overline{\text{MS}}}^{(N_F)})$ and β_i are the $\overline{\text{MS}}$ -scheme coefficients listed e.g. in [23].

We take into account bottom mass effects by retaining the massless $N_F = 5$ expressions and adding the difference between the massless and massive LO and NLO coefficients A and B [46, 47, 48, 49], where a pole b-quark mass of $m_b = 4.5 \text{ GeV}$ was used.

In the limit $y \rightarrow 0$ one observes that the perturbative contribution of order α_s^n to the cross section diverges like $\alpha_s^n L^{2n}$, with $L = -\ln y$ ($L = -\ln(y/6)$ for $y = C$). This leading logarithmic (LL) behaviour is due to multiple soft gluon emission at higher orders, and the LL coefficients exponentiate, such that they can be resummed to all orders. For the event-shape observables considered here, and assuming massless quarks, the next-to-leading logarithmic (NLL) corrections can also be resummed to all orders in the coupling constant.

In order to obtain a reliable description of the event-shape distributions over a wide range in y , it is mandatory to combine fixed order and resummed predictions. However, in order to avoid the double counting of terms common to both, the two predictions have to be matched onto each other. A number of different matching procedures have been proposed in the literature, see e.g. Ref. [50] for a review.

The most commonly used procedure is the so-called $\ln R$ -matching [18], which we used in two different variants for our study on α_s [27]. For more details about the NLLA+NNLO matching we refer the reader to Ref. [26].

2.2 Moments of event-shape observables

The n th moment of an event-shape observable y is defined by

$$\langle y^n \rangle = \frac{1}{\sigma_{\text{had}}} \int_0^{y_{\text{max}}} y^n \frac{d\sigma}{dy} dy, \quad (4)$$

where y_{max} is the kinematically allowed upper limit of the observable. For moments of event shapes, one expects the hadronisation corrections to be additive, such that they can be divided into a perturbative and a non-perturbative contribution,

$$\langle y^n \rangle = \langle y^n \rangle_{\text{pt}} + \langle y^n \rangle_{\text{np}}, \quad (5)$$

where the non-perturbative contribution accounts for hadronisation effects.

In ref. [34], the dispersive model derived in Refs. [35, 36, 37, 38] has been used to estimate hadronisation corrections to event-shape moments by calculating analytical predictions for power corrections. It introduces only a single new parameter α_0 , which can be interpreted as the average strong coupling in the non-perturbative region:

$$\frac{1}{\mu_I} \int_0^{\mu_I} dQ \alpha_{\text{eff}}(Q^2) = \alpha_0(\mu_I), \quad (6)$$

where below the IR cutoff μ_I the strong coupling is replaced by an effective coupling. This dispersive model for the strong coupling leads to a shift in the distributions

$$\frac{d\sigma}{dy}(y) = \frac{d\sigma_{\text{pt}}}{dy}(y - a_y P), \quad (7)$$

where the numerical factor a_y depends on the event shape, while P is believed to be universal and scales with the centre-of-mass energy like μ_I/Q . Insertion of eq. (7) into the definition of the moments leads to

$$\begin{aligned} \langle y^n \rangle &= \int_{-a_y P}^{y_{\text{max}} - a_y P} dy (y + a_y P)^n \frac{1}{\sigma_{\text{tot}}} \frac{d\sigma_{\text{pt}}}{dy}(y) \\ &\approx \int_0^{y_{\text{max}}} dy (y + a_y P)^n \frac{1}{\sigma_{\text{tot}}} \frac{d\sigma_{\text{pt}}}{dy}(y). \end{aligned} \quad (8)$$

From this expression one can extract the non-perturbative predictions for the moments of y . To combine the dispersive model with the perturbative prediction at NNLO QCD, the analytical expressions have been extended [34] to compensate for all scale-dependent terms at this order.

3. DETERMINATION OF α_s AND α_0

3.1 α_s from distributions of hadronic event shapes

We have used the six event-shape observables listed in section 2. for our fits. The measurements we use have been carried out by the ALEPH collaboration [1] at eight different centre-of-mass energies between 91.2 and 206 GeV. The event-shape distributions were obtained from the reconstructed momenta and energies of charged and neutral particles. The measurements have been corrected for detector effects, i.e. the final distributions correspond to the so-called particle (or hadron) level. In addition, at LEP2 energies above the Z peak they were corrected for initial-state radiation effects. At energies above 133 GeV, backgrounds from 4-fermion processes, mainly from W-pair production and also ZZ and Z γ^* ,

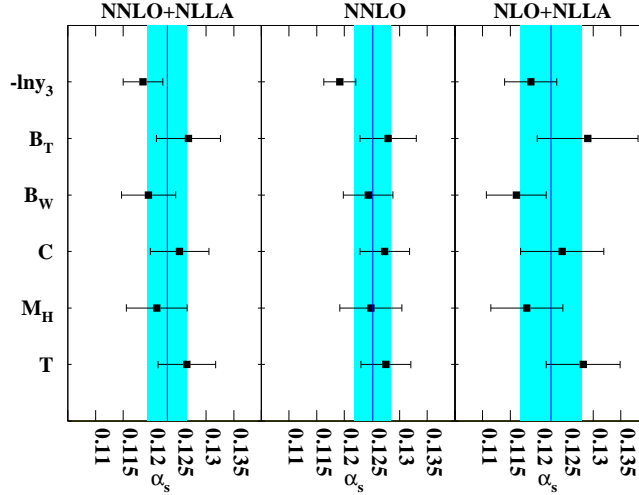


Fig. 1: The measurements of the strong coupling constant α_s for the six event shapes, at $\sqrt{s} = M_Z$, when using QCD predictions at different approximations in perturbation theory. The shaded area corresponds to the total uncertainty.

were subtracted following the procedure given in [1]. The experimental uncertainties were estimated by varying event and particle selection cuts. They are below 1% at LEP1 and slightly larger at LEP2.

The perturbative QCD prediction is corrected for hadronisation and resonance decays by means of a transition matrix, which is computed with the Monte Carlo generators PYTHIA [51], HERWIG [52] and ARIADNE [53], all tuned to global hadronic observables at M_Z [54]. The parton level is defined by the quarks and gluons present at the end of the parton shower in PYTHIA and HERWIG and the partons resulting from the colour dipole radiation in ARIADNE. Corrected measurements of event-shape distributions are compared to the theoretical calculation at particle level. For a detailed description of the determination and treatment of experimental systematic uncertainties we refer to Refs. [1, 25].

We also made studies using the NLO+LL event generator HERWIG++ [55], which will be described in more detail below.

The value of α_s is determined at each energy using a binned least-squares fit. The fit programs of Ref. [25] have been extended to incorporate the NNLO+NLLA calculations. Combining the results for six event-shape variables and eight LEP1/LEP2 centre-of-mass energies, we obtain

$$\alpha_s(M_Z) = 0.1224 \pm 0.0009 (\text{stat}) \pm 0.0009 (\text{exp}) \pm 0.0012 (\text{had}) \pm 0.0035 (\text{theo}) .$$

The fitted values of the coupling constant as found from event-shape variables calculated at various orders are shown in Fig. 1. Comparing our results to both the fit using purely fixed-order NNLO predictions [25] and the fits based on earlier NLLA+NLO calculations [1], we make the following observations:

- The central value is slightly lower than the central value of 0.1228 obtained from fixed-order NNLO only, and slightly larger than the NLO+NLLA results. The fact that the central value is almost identical to the purely fixed-order NNLO result could be anticipated from the findings in Ref. [26]. There it is shown that in the three-jet region, which provides the bulk of the fit range, the matched NLLA+NNLO prediction is very close to the fixed-order NNLO calculation.
- The dominant theoretical uncertainty on $\alpha_s(M_Z)$, as estimated from scale variations, is reduced by 20% compared to NLO+NLLA. However, compared to the fit based on purely fixed-order NNLO predictions, the perturbative uncertainty is *increased* in the NNLO+NLLA fit. The reason is that in

the two-jet region the NLLA+NLO and NLLA+NNLO predictions agree by construction, because the matching suppresses any fixed order terms. Therefore, the renormalisation scale uncertainty is dominated by the next-to-leading-logarithmic approximation in this region, which results in a larger overall scale uncertainty in the α_s fit.

- As already observed for the fixed-order NNLO results, the scatter among the values of $\alpha_s(M_Z)$ extracted from the six different event-shape variables is substantially reduced compared to the NLO+NLLA case.
- The matching of NLLA+NNLO introduces a mismatch in the cancellation of renormalisation scale logarithms, since the NNLO expansion fully compensates the renormalisation scale dependence up to two loops, while NLLA only compensates it up to one loop. In order to assess the impact of this mismatch, we have introduced the $\ln R(\mu)$ matching scheme [27], which retains the two-loop renormalisation terms in the resummed expressions and the matching coefficients. In this scheme, a substantial reduction of the perturbative uncertainty from ± 0.0035 (obtained in the default $\ln R$ -scheme) to ± 0.0022 is observed, which might indicate the size of the ultimately reachable precision for a complete NNLO+NNLLA calculation. Although both schemes are in principle on the same theoretical footing, it is the more conservative error estimate obtained in the $\ln R$ -scheme which should be taken as the nominal value, since it measures the potential impact of the yet uncalculated finite NNLLA-terms.
- Bottom quark mass effects, which are numerically significant mainly at the LEP1 energy, were included through to NLO. Compared to a purely massless evaluation of the distributions, the inclusion of these mass effects enhances $\alpha_s(M_Z)$ by 0.8%.

Hadronisation corrections from LL+NLO event generators

In recent years large efforts went into the development of modern Monte Carlo event generators which include in part NLO corrections matched to parton showers at leading logarithmic accuracy (LL) for various processes. Here we use HERWIG++ [55, 56] version 2.3 for our investigations. Several schemes for the implementation of NLO corrections are available [57, 58, 59]. We studied the MCNLO [57] and POWHEG [58] schemes¹.

We compared the prediction for the event-shape distributions of HERWIG++ to both the high precision data at LEP1 from ALEPH and the predictions from the legacy generators PYTHIA, HERWIG and ARIADNE. We recall that the latter have all been tuned to the same global QCD observables measured by ALEPH [54] at LEP1, which included event-shape variables similar to the ones analysed here. To investigate the origin of the observed differences between the generators, we decided to consider the parton-level predictions and the hadronisation corrections separately. Discussing the full details of our study is beyond the scope of this note; here we only mention some of our observations. HERWIG++ with POWHEG yields a similar shape as the legacy programs, but differs in the normalisation. The other HERWIG++ predictions differ most notably in shape from the former. The fit quality of HERWIG++ with POWHEG is similar to the outcome of the legacy generators. Given the similar shape but different normalisation of HERWIG++ with POWHEG, the resulting values of α_s are significantly lower, overall by 3%. For further details we refer to Ref. [27].

From the study of hadronisation corrections we make the following important observation. It appears that there are two “classes” of variables. The first class contains thrust, C-parameter and total jet broadening, while the second class consists of the heavy jet mass, wide jet broadening and the two-to-three-jet transition parameter Y_3 . For the first class, using the standard hadronisation corrections from PYTHIA, we obtain $\alpha_s(M_Z)$ values around 0.125 – 0.127, some 5% higher than those found from the second class of variables. In a study of higher moments of event shapes [32], indications were found that variables from the first class still suffer from sizable missing higher order corrections, whereas the

¹We use the notation MCNLO for the *method*, while MC@NLO denotes the *program*.

second class of observables have a better perturbative stability. In Ref. [27], we observed that this first class of variables gives a parton level prediction with PYTHIA, which is about 10% higher than the NNLO+NLLA prediction. The PYTHIA result is obtained with tuned parameters, where the tuning to data had been performed at the hadron level. This tuning results in a rather large effective coupling in the parton shower, which might partly explain the larger parton level prediction of PYTHIA. As the tuning has been performed at hadron level, this implies that the hadronisation corrections come out to be smaller than what would have been found by tuning a hypothetical Monte Carlo prediction with a parton level corresponding to the NNLO+NLLA prediction. This means that the PYTHIA hadronisation corrections, applied in the α_s fit, might be too small, resulting in a larger $\alpha_s(M_Z)$ value. Since up to now the hadronisation uncertainties have been estimated from the differences of parton shower based models, tuned to the data, it is likely that for these event shapes the uncertainties were underestimated, missing a possible systematic shift. Such problems do not appear to exist for the second class of variables.

We would like to mention that a determination of α_s based on 3-jet rates calculated at NNLO accuracy also has been performed recently [60], with the result $\alpha_s(M_Z) = 0.1175 \pm 0.0020(\text{exp}) \pm 0.0015(\text{theo})$, which is also lower than the one obtained from fits to distributions of event shapes.

3.2 α_s and α_0 from moments of hadronic event shapes

Now we turn to analytical models to estimate hadronisation corrections. The expressions derived in [34] match the dispersive model with the perturbative prediction at NNLO QCD. Comparing these expressions with experimental data on event-shape moments, a combined determination of the perturbative strong coupling constant α_s and the non-perturbative parameter α_0 has been performed [34], based on data from the JADE and OPAL experiments [17]. The data consist of 18 points at centre-of-mass energies between 14.0 and 206.6 GeV for the first five moments of T , C , Y_3 , M_H , B_W and B_T , and have been taken from [61]. For each moment the NLO as well as the NNLO prediction was fitted with $\alpha_s(M_Z)$ and α_0 as fit parameters, except for the moments of Y_3 , which have no power correction and thus are independent of α_0 .

Compared to previous results at NLO, inclusion of NNLO effects results in a considerably improved consistency in the parameters determined from different shape variables, and in a substantial reduction of the error on α_s .

We further observe that the theoretical error on the extraction of $\alpha_s(M_Z)$ from ρ , Y_3 and B_W is considerably smaller than from τ , C and B_T . As mentioned above and discussed in detail in [32], the moments of the former three shape variables receive moderate NNLO corrections for all n , while the NNLO corrections for the latter three are large already for $n = 1$ and increase with n . Consequently, the theoretical description of the moments of ρ , Y_3 and B_W displays a higher perturbative stability, which is reflected in the smaller theoretical uncertainty on $\alpha_s(M_Z)$ derived from those variables.

In a second step, we combine the $\alpha_s(M_Z)$ and α_0 measurements obtained from different event-shape variables. Taking the weighted mean over all values except B_W and B_T , we obtain at NNLO:

$$\begin{aligned}\alpha_s(M_Z) &= 0.1153 \pm 0.0017(\text{exp}) \pm 0.0023(\text{th}), \\ \alpha_0 &= 0.5132 \pm 0.0115(\text{exp}) \pm 0.0381(\text{th}),\end{aligned}\tag{9}$$

The moments of B_W and B_T have been excluded here since their theoretical description requires an additional contribution to the non-perturbative coefficient P (see eq. (7)) which is not available consistently to NNLO.

To illustrate the improvement due to the inclusion of the NNLO corrections, we also quote the corresponding NLO results. Based on τ , C , ρ and Y_3 , we obtain:

$$\begin{aligned}\alpha_s^{\text{NLO}}(M_Z) &= 0.1200 \pm 0.0021(\text{exp}) \pm 0.0062(\text{th}), \\ \alpha_0^{\text{NLO}} &= 0.4957 \pm 0.0118(\text{exp}) \pm 0.0393(\text{th}),\end{aligned}$$

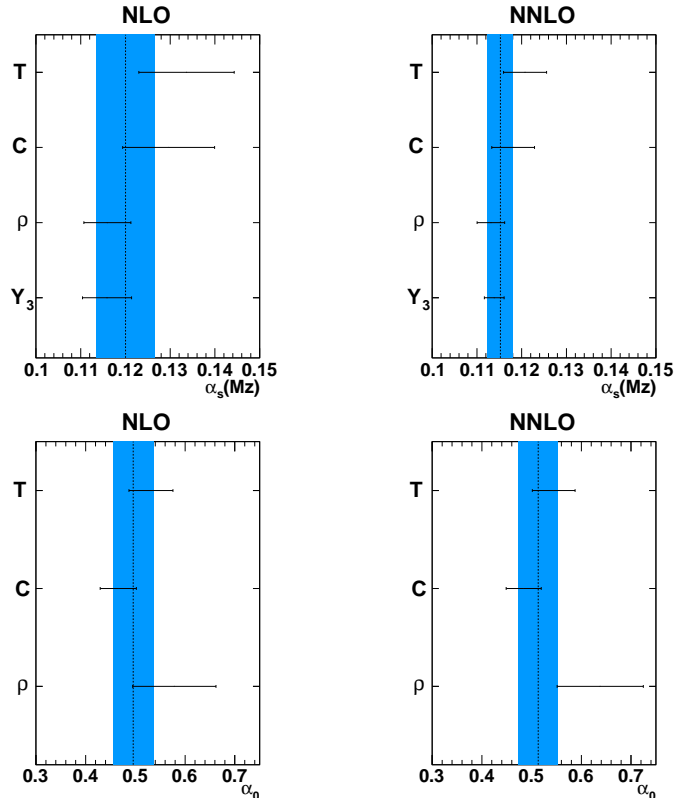


Fig. 2: Error bands at NLO and NNLO for combinations of values for α_s and α_0 obtained from fits to moments of different event shapes. The error on α_s is dominated by scale uncertainties, while the largest contribution to the error on α_0 comes from the uncertainty on the Milan factor.

We compare the NLO and NNLO combinations in Figure 2. It can be seen very clearly that the measurements obtained from the different variables are consistent with each other within errors. The average of $\alpha_s(M_Z)$ is dominated by the measurements based on ρ and Y_3 , which have the smallest theoretical uncertainties. From NLO to NNLO, the error on $\alpha_s(M_Z)$ is reduced by a factor of two. Analysing the different sources of the systematical errors, we observe that the error on $\alpha_s(M_Z)$ is clearly dominated by the x_μ variation, while the largest contribution to the error on α_0 comes from the uncertainty on the Milan factor \mathcal{M} [37]. Since this uncertainty has not been improved in the current study, it is understandable that the systematic error on α_0 remains unchanged.

To quantify the difference of the dispersive model to hadronisation corrections from the legacy generators, we analysed the moments of (1-T) with hadronisation corrections from PYTHIA. As a result, we obtained fit results for $\alpha_s(M_Z)$ which are typically 4% higher than by using the dispersive model, with a slightly worse quality of the fit. Comparing perturbative and non-perturbative contributions at $\sqrt{s} = M_Z$, we observed that PYTHIA hadronisation corrections amount to less than half the power corrections obtained in the dispersive model, thereby explaining the tendency towards a larger value of $\alpha_s(M_Z)$, since the missing numerical magnitude of the power corrections must be compensated by a larger perturbative contribution.

CONCLUSIONS

We have compared determinations of the strong coupling constant based on hadronic event shapes measured at LEP using two different approaches:

1. a fit of perturbative QCD results at next-to-next-to-leading order (NNLO), matched to resummation

in the next-to-leading-logarithmic approximation (NLLA), to ALEPH data where the hadronisation corrections have been estimated using Monte Carlo event generators

2. a fit of perturbative QCD results at NNLO matched to non-perturbative power corrections in the dispersive model, providing analytical parametrisations of hadronisation corrections, to JADE and OPAL data.

We find that the second approach results in a considerably lower value of $\alpha_s(M_Z)$ than the first one.

We conclude that apparently there are two “classes” of event-shape variables, the first class containing thrust, C-parameter and total jet broadening, the second class containing heavy jet mass, wide jet broadening and the two-to-three-jet transition parameter Y_3 . Comparing parton level and hadron level predictions from PYTHIA, this first class of variables gives a parton level prediction which is about 10% higher than the NNLO+NLLA prediction, where the PYTHIA curve has been obtained with tuned parameters, the tuning to data being performed at the hadron level. This tuning results in a rather large effective coupling in the parton shower, such that the parton level prediction of PYTHIA turns out large. This may imply that the hadronisation corrections come out to be too small for these variables, resulting in a larger $\alpha_s(M_Z)$ value. This hypothesis is corroborated by the fact that the theoretical description of the moments of the variables thrust, C-parameter and total jet broadening displays a lower perturbative stability.

For the moments of (1-T), we found that the legacy generators predict power corrections which are less than half of what is obtained in the dispersive model. The large numerical discrepancy between analytical power corrections and the estimate of hadronisation effects from the legacy generators suggests to revisit the impact of hadronisation corrections on precision QCD observables.

ACKNOWLEDGEMENTS

This research was supported in part by the Swiss National Science Foundation (SNF) under contracts PP0022-118864 and 200020-126691, by the UK Science and Technology Facilities Council, by the European Commission’s Marie-Curie Research Training Network MRTN-CT-2006-035505 and by the German Helmholtz Alliance “Physics at the Terascale”.

References

- [1] A. Heister *et. al.*, **ALEPH** Collaboration *Eur. Phys. J.* **C35** (2004) 457–486.
- [2] D. Buskulic *et. al.*, **ALEPH** Collaboration *Z. Phys.* **C73** (1997) 409–420.
- [3] P. D. Acton *et. al.*, **OPAL** Collaboration *Z. Phys.* **C59** (1993) 1–20.
- [4] G. Alexander *et. al.*, **OPAL** Collaboration *Z. Phys.* **C72** (1996) 191–206.
- [5] K. Ackerstaff *et. al.*, **OPAL** Collaboration *Z. Phys.* **C75** (1997) 193–207.
- [6] G. Abbiendi *et. al.*, **OPAL** Collaboration *Eur. Phys. J.* **C16** (2000) 185–210.
- [7] G. Abbiendi *et. al.*, **OPAL** Collaboration *Eur. Phys. J.* **C40** (2005) 287–316.
- [8] M. Acciarri *et. al.*, **L3** Collaboration *Phys. Lett.* **B371** (1996) 137–148.
- [9] M. Acciarri *et. al.*, **L3** Collaboration *Phys. Lett.* **B404** (1997) 390–402.
- [10] M. Acciarri *et. al.*, **L3** Collaboration *Phys. Lett.* **B444** (1998) 569–582.
- [11] P. Achard *et. al.*, **L3** Collaboration *Phys. Lett.* **B536** (2002) 217–228.
- [12] P. Achard *et. al.*, **L3** Collaboration *Phys. Rept.* **399** (2004) 71–174.

- [13] P. Abreu *et. al.*, **DELPHI** Collaboration *Phys. Lett.* **B456** (1999) 322–340.
- [14] J. Abdallah *et. al.*, **DELPHI** Collaboration *Eur. Phys. J.* **C29** (2003) 285–312.
- [15] J. Abdallah *et. al.*, **DELPHI** Collaboration *Eur. Phys. J.* **C37** (2004) 1–23.
- [16] P. A. Movilla Fernandez, O. Biebel, S. Bethke, S. Kluth, and P. Pfeifenschneider,, **JADE** Collaboration *Eur. Phys. J.* **C1** (1998) 461–478, [hep-ex/9708034].
- [17] C. Pahl, S. Bethke, S. Kluth, J. Schieck, and t. J. collaboration, *Eur. Phys. J.* **C60** (2009) 181–196, [0810.2933].
- [18] S. Catani, L. Trentadue, G. Turnock, and B. R. Webber, *Nucl. Phys.* **B407** (1993) 3–42.
- [19] R. K. Ellis, D. A. Ross, and A. E. Terrano, *Nucl. Phys.* **B178** (1981) 421.
- [20] Z. Kunszt, *Phys. Lett.* **B99** (1981) 429.
- [21] Z. Kunszt and P. Nason,, Z Physics at LEP 1, CERN Yellow Report 89-08, Vol. 1, p. 373.
- [22] A. Gehrmann-De Ridder, T. Gehrmann, E. W. N. Glover, and G. Heinrich, *Phys. Rev. Lett.* **99** (2007) 132002, [0707.1285].
- [23] A. Gehrmann-De Ridder, T. Gehrmann, E. W. N. Glover, and G. Heinrich, *JHEP* **12** (2007) 094, [0711.4711].
- [24] S. Weinzierl, *JHEP* **06** (2009) 041, [0904.1077].
- [25] G. Dissertori *et. al.*, *JHEP* **02** (2008) 040, [0712.0327].
- [26] T. Gehrmann, G. Luisoni, and H. Stenzel, *Phys. Lett.* **B664** (2008) 265–273, [0803.0695].
- [27] G. Dissertori *et. al.*, *JHEP* **08** (2009) 036, [0906.3436].
- [28] A. Denner, S. Dittmaier, T. Gehrmann, and C. Kurz, *Phys. Lett.* **B679** (2009) 219–222, [0906.0372].
- [29] S. Bethke, S. Kluth, C. Pahl, and J. Schieck,, **JADE** Collaboration *Eur. Phys. J.* **C64** (2009) 351–360, [0810.1389].
- [30] R. A. Davison and B. R. Webber, *Eur. Phys. J.* **C59** (2009) 13–25, [0809.3326].
- [31] T. Becher and M. D. Schwartz, *JHEP* **07** (2008) 034, [0803.0342].
- [32] A. Gehrmann-De Ridder, T. Gehrmann, E. W. N. Glover, and G. Heinrich, *JHEP* **05** (2009) 106, [0903.4658].
- [33] S. Weinzierl, *Phys. Rev.* **D80** (2009) 094018, [0909.5056].
- [34] T. Gehrmann, M. Jaquier, and G. Luisoni, 0911.2422.
- [35] Y. L. Dokshitzer, G. Marchesini, and B. R. Webber, *Nucl. Phys.* **B469** (1996) 93–142, [hep-ph/9512336].
- [36] Y. L. Dokshitzer and B. R. Webber, *Phys. Lett.* **B404** (1997) 321–327, [hep-ph/9704298].
- [37] Y. L. Dokshitzer, A. Lucenti, G. Marchesini, and G. P. Salam, *JHEP* **05** (1998) 003, [hep-ph/9802381].

- [38] Y. L. Dokshitzer, G. Marchesini, and G. P. Salam, *Eur. Phys. J. direct* **C1** (1999) 3, [hep-ph/9812487].
- [39] E. Farhi, *Phys. Rev. Lett.* **39** (1977) 1587–1588.
- [40] L. Clavelli and D. Wyler, *Phys. Lett.* **B103** (1981) 383.
- [41] P. E. L. Rakow and B. R. Webber, *Nucl. Phys.* **B191** (1981) 63.
- [42] G. Parisi, *Phys. Lett.* **B74** (1978) 65.
- [43] J. F. Donoghue, F. E. Low, and S.-Y. Pi, *Phys. Rev.* **D20** (1979) 2759.
- [44] W. J. Stirling, *J. Phys.* **G17** (1991) 1567–1574.
- [45] S. Bethke, Z. Kunszt, D. E. Soper, and W. J. Stirling, *Nucl. Phys.* **B370** (1992) 310–334.
- [46] A. Brandenburg and P. Uwer, *Nucl. Phys.* **B515** (1998) 279–320, [hep-ph/9708350].
- [47] W. Bernreuther, A. Brandenburg, and P. Uwer, *Phys. Rev. Lett.* **79** (1997) 189–192, [hep-ph/9703305].
- [48] G. Rodrigo, A. Santamaria, and M. S. Bilenky, *Phys. Rev. Lett.* **79** (1997) 193–196, [hep-ph/9703358].
- [49] P. Nason and C. Oleari, *Nucl. Phys.* **B521** (1998) 237–273, [hep-ph/9709360].
- [50] R. W. L. Jones, M. Ford, G. P. Salam, H. Stenzel, and D. Wicke, *JHEP* **12** (2003) 007, [hep-ph/0312016].
- [51] T. Sjostrand *et. al.*, *Comput. Phys. Commun.* **135** (2001) 238–259, [hep-ph/0010017].
- [52] G. Corcella *et. al.*, *JHEP* **01** (2001) 010, [hep-ph/0011363].
- [53] L. Lonnblad, *Comput. Phys. Commun.* **71** (1992) 15–31.
- [54] R. Barate *et. al.*, **ALEPH** Collaboration *Phys. Rept.* **294** (1998) 1–165.
- [55] O. Latunde-Dada, *JHEP* **11** (2007) 040, [0708.4390].
- [56] O. Latunde-Dada, S. Gieseke, and B. Webber, *JHEP* **02** (2007) 051, [hep-ph/0612281].
- [57] S. Frixione and B. R. Webber, *JHEP* **06** (2002) 029, [hep-ph/0204244].
- [58] P. Nason, *JHEP* **11** (2004) 040, [hep-ph/0409146].
- [59] K. Hamilton, P. Richardson, and J. Tully, *JHEP* **11** (2009) 038, [0905.3072].
- [60] G. Dissertori *et. al.*, 0910.4283.
- [61] C. J. Pahl, Ph.D. thesis, MPI Munich 2007.